Journal of Hazardous Materials 164 (2009) 615–620

Contents lists available at ScienceDirect

Journal of Hazardous Materials

journal homepage: www.elsevier.com/locate/jhazmat

Photodegradation of rhodamine B under visible light by bimetal codoped TiO_2 nanocrystals

Zhuyi Wang, Cheng Chen, Fengqing Wu*, Bo Zou, Meng Zhao, Jinxing Wang, Caihui Feng

College of Chemistry, Jilin University, Changchun 130023, China

ARTICLE INFO

Article history:
Received 7 February 2008
Received in revised form 14 August 2008
Accepted 14 August 2008
Available online 22 August 2008

Keywords:
TiO_2
Codoped
Stearic acid gel method
Photocatalysis
Rhodamine B

ABSTRACT

In the search for efficient photocatalysts working under visible light, we have investigated the effect of metal ions (Bi/Co, Fe/Co) codoping on the photocatalytic activity of TiO_2 prepared by stearic acid gel method. UV–vis spectra revealed that doped Co enhanced the absorbency of TiO_2 under visible light, and Bi/Co codoped TiO_2 showed higher absorbance than Fe/Co codoped TiO_2. The photoreaction based on the prepared samples for photodegradation of 20 mg/l rhodamine B solution was examined. The results showed that Fe(0.1%)/Co(0.4%) codoped TiO_2 had the highest photoactivity among all as-prepared samples under visible light, though less absorbency of visible light, indicating that the photoactivity not only benefits from absorbency but also relates to the cooperative effect of the two dopants.

1. Introduction

Dye pollutants are important sources of environmental contamination. They can be effectively removed in wastewater by the photocatalytic process of semiconductor photocatalysts. Up to date, remarkable progresses have been made in the photodegradation of dye pollutants under ultraviolet (UV) light, but less effort in the visible light. Therefore, effective utilization of visible light to degrade dye pollutants from the viewpoint of using the solar energy is an attractive attempt [1].

Semiconductor photocatalysts such as CdS, ZnS, CdSe, etc. [2–3] have been studied extensively due to their ideal edge positions of the valence and conduction bands for the oxidation and reduction. One of the disadvantages of this type of photocatalysts is photocorrosion [4], i.e. CdS, ZnS, and CdSe are oxidized into ions by the hole produced in its valence band by itself. TiO_2 as a semiconductor catalyst is widely used in the photodegradation process because it is cheap, stable, nontoxic, and exhibits strong photoactivity. However, its band gap (3.0–3.2 eV) can only capture UV light. To extend the response of TiO_2 to visible light, the modified TiO_2 systems by doping have been considered [5–9]. Many researches have focused on doping some transition metals or nonmetal elements in TiO_2. Some groups have attempted to dope two kinds of elements in TiO_2, i.e. codoping [10–23]. Nevertheless, codoping two transition metal ions in TiO_2 to improve its photoactivity under visible light was rarely reported [23].

In this paper, Fe(III)/Co(II) and Bi(III)/Co(II) were codoped into TiO_2 by stearic acid gel method, and the photocatalytic properties of as-prepared samples were evaluated with 20 mg/L rhodamine B (RB, $C_{28}H_{31}N_2O_3Cl$), a xanthene dye, under UV and visible light.

2. Experimental

2.1. Preparation of catalysts

The doped TiO_2 nanocrystals were prepared by adding titanium tetraisopropoxide (CP, 2.5 ml) to the melting stearic acid (AR, 10 g) with vigorous stirring at 70 °C, and then metal acetates (CP) were added to the mixture. The molar concentrations of monodoped Fe(III), Co(II) or Bi(III) in TiO_2 were controlled to be 0.5%, and codoped Fe(III)/Co(II) or Bi(III)/Co(II) in TiO_2 were controlled to be 0.1%:0.4%, 0.25%:0.25%, 0.4%:0.1%, and 0.5%:0.5%. After 2 h, the mixture was cooled down in cold water, then combusted in air at 300 °C, and subsequently calcined at 450 °C for 2 h in atmosphere.

2.2. Characterization of catalysts

X-ray powder diffraction (XRD) analysis was carried out using a Shimadzu LabX XRD-6000. Specific surface areas were measured by the BET method employing a nitrogen adsorption–desorption analyzer (Quantachrome Autosorb-1C). Scanning electron microscopy (SEM) studies were performed with a JEOL JSM-6700F. UV–vis dif-

* Corresponding author. Tel.: +86 431 85168397.
E-mail address: fqwu@mail.jlu.edu.cn (F. Wu).

0304-3894/$ – see front matter.
doi:10.1016/j.jhazmat.2008.08.041

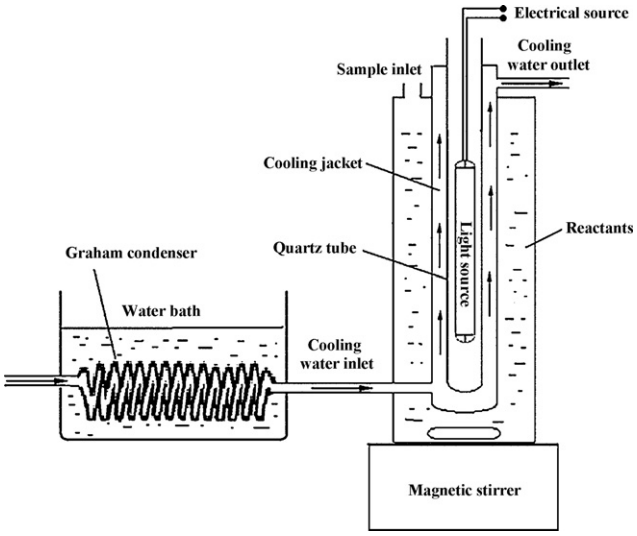

Fig. 1. Schematic diagram of the photoreactor.

fuse reflectance spectra analysis was performed with Perkin–Elmer Lambda 20.

2.3. Photochemical reaction

The experiment was performed in a jacketed column quartz reactor (700 ml). The schematic diagram of photoreactor is shown in Fig. 1. The UV light source was obtained through high pressure Hg lamp (300 W) with an emission wavelength range from 320 to 450 nm centered at 365 nm. The artificial visible light source was obtained through Xe lamp (500 W) with an emission wavelength range from 290 to 800 nm, and $NaNO_2$ solution was circulated through the cooling jacket to filter out the UV emission of the lamp below 400 nm. The lamp was put in a quartz tube and then placed inside the reactor. The reaction temperature was maintained at 25 °C by cooling water in the cooling jacket of the reactor. The initial concentration of RB was 20 mg/L and the catalyst was 1.0 g/L. After stirring magnetically in the dark for 30 min, the light was turned on and it was treated as the starting point ($t = 0$) of the reaction, where the concentration of RB was designed as C_0. The sample solutions were collected at regular intervals for subsequent analysis by a Shimadzu UV-2450 spectrophotometer to determine the concentration of RB (C) at the time, the sampling volume was 2 ml each time. The maximum absorption wavelength for the measurement of RB was found to be 554 nm, the RB concentration was calculated by the calibration curve of RB concentration at wavelength of 554 nm.

Table 1
The crystal size, percent of rutile and BET surface area of samples

Sample	I_R/I_A	Percent of rutile (%)	Crystal size (nm)	BET (m^2/g)
Undoped TiO_2	0.11	11.7	11.8	91.3
Fe(0.5%)	0.09	9.7	12.8	74.1
Fe(0.4%)/Co(0.1%)	0.14	14.4	10.5	108.5
Fe(0.25%)/Co(0.25%)	0.09	9.7	11.7	
Fe(0.1%)/Co(0.4%)	0.10	10.7	11.4	91.0
Co(0.5%)	0.09	9.7	12.1	72.6
Fe(0.5%)/Co(0.5%)	0.14	14.4	12.5	
Bi(0.5%)	0.12	12.6	11.6	79.2
Bi(0.4%)/Co(0.1%)	0.08	8.8	10.6	
Bi(0.25%)/Co(0.25%)	0.09	9.7	11.3	93.2
Bi(0.1%)/Co(0.4%)	0.07	7.7	11.2	
Co(0.5%)	0.09	9.7	12.1	72.6
Bi(0.5%)/Co(0.5%)	0.08	8.8	10.2	105.7

3. Results and discussions

3.1. Characterization of photocatalysts

XRD is used to investigate the phase structure of the samples. The characteristic peaks of rutile and anatase are indicated in Fig. 2. No additional peaks except for the TiO_2 are observed, this may be due to the small amount of dopants or their high dispersion in samples. The peak at 25.4° was used to calculate the average crystal size by Scherrer equation. The crystal sizes of all samples shown in Table 1 are about 11 nm, which demonstrates that the samples consist of nanocrystals and the doped ion has no obvious influence on their crystal sizes.

Comparing the characteristic peak intensities of the rutile (27.4°) and the anatase (25.4°) forms revealed that all as-prepared samples had similar intensity ratio I_R/I_A (Table 1) of the two crystal phases. In general, the intensity of characteristic peaks is proportional to the content of corresponding crystal phases. Similar intensity ratio means that the doped ion has no obvious influence on the percent of two phases. It also can be found from Table 1 that the surface areas of samples were around 90 m^2/g.

The morphology of the samples was detected by using a scanning electron microscopy (SEM). The SEM micrographs of the samples (Fig. 3) show that the samples consist of agglomerated particles, and the amounts of doped metal ions had not obvious influence on the morphology of the samples.

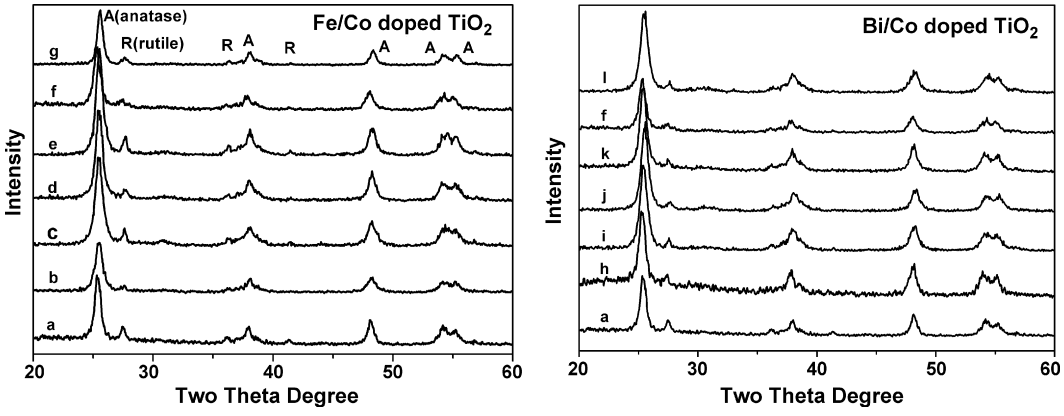

Fig. 2. XRD patterns of as-prepared samples ((a) undoped TiO_2, (b) Fe(0.5%)-TiO_2, (c) Fe(0.4%)/Co(0.1%)-TiO_2, (d) Fe(0.25%)/Co(0.25%)-TiO_2, (e) Fe(0.1%)/Co(0.4%)-TiO_2, (f) Co(0.5%)-TiO_2, (g) Fe(0.5%)/Co(0.5%)-TiO_2, (h) Bi(0.5%)-TiO_2, (i) Bi(0.4%)/Co(0.1%)-TiO_2, (j) Bi(0.25%)/Co(0.25%)-TiO_2, (k) Bi(0.1%)/Co(0.4%)-TiO_2, (l) Bi(0.5%)/Co(0.5%)-TiO_2).

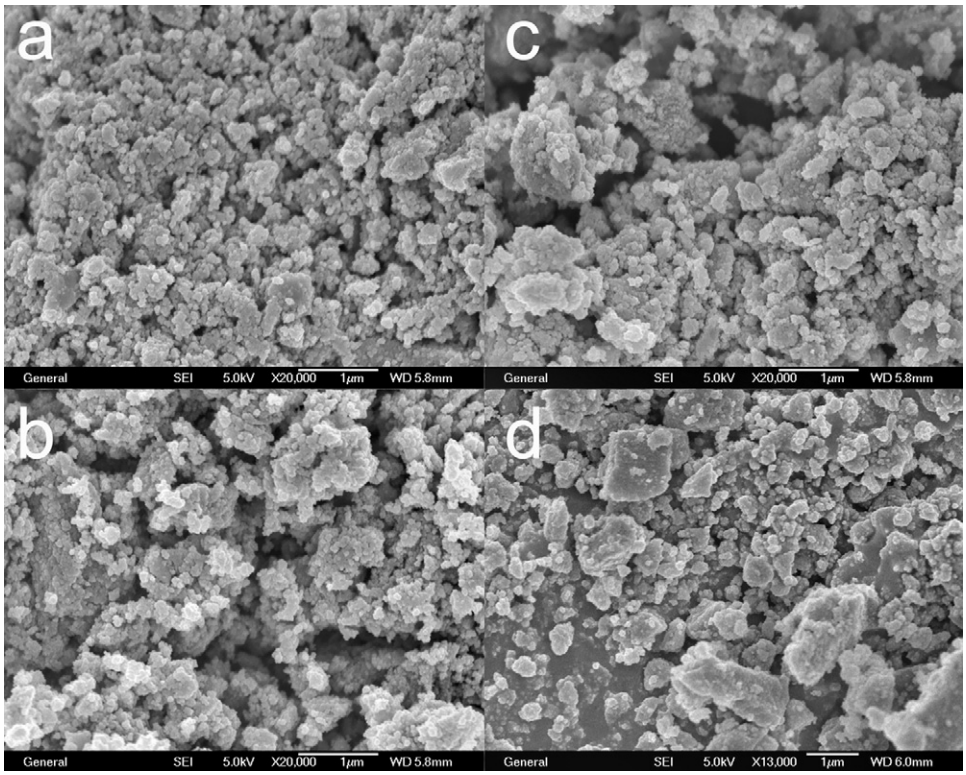

Fig. 3. SEM micrographs of ((a) Fe(0.5%)-TiO_2, (b) Fe(0.4%)/Co(0.1%)-TiO_2, (c) Fe(0.1%)/Co(0.4%)-TiO_2, (d) Fe(0.5%)/Co(0.5%)-TiO_2).

Fig. 4 shows the UV–vis absorption spectra of as-prepared samples. The Co-monodoped TiO_2 (curve f) absorbed a larger amount of visible light than the undoped TiO_2 (curve a), and Fe or Bi-monodoped TiO_2 (curve *b*, h), indicating that the doped Co in TiO_2 induced intense absorbency of visible light. Fe/Co codoped TiO_2 showed the lower absorbency than Co monodoped TiO_2, and Bi/Co codoped TiO_2 exhibited the higher absorbency than Co monodoped TiO_2. The absorbency of as-prepared samples in the visible light region followed the order: Bi/Co codoped TiO_2 > Co monodoped TiO_2 > Fe/Co codoped TiO_2; the results may be explained by the cooperative effect of the two metal ion dopants in the photoabsorption.

3.2. Photocatalytic performance

The degradation profiles for Fe/Co doped TiO_2 under UV and visible light are shown in Fig. 5. As can be seen from Fig. 5(a), apart from Co(0.5%)-TiO_2 and Fe(0.1%)/Co(0.4%)-TiO_2, all the other samples showed lower photoactivity than undoped TiO_2, even though in the presence of Co(0.5%)-TiO_2 and Fe(0.1%)/Co(0.4%)-TiO_2, almost 70% RB was still remained in the solution under illumination for 3 h, which implied that the photoactivity of samples under UV did not benefit from Fe/Co doping. It was supposed that when doping excess concentration of Fe, small agglomerations of Fe_2O_3 formed at the surface of TiO_2 particles, which would result in the decrease of photoactivity [24].

But the photoreaction of Fe/Co doped TiO_2 under visible light showed relatively satisfying results (Fig. 5(b)). In the absence of the photocatalysts, no observable degradation of the dye occurred. In the presence of photocatalysts, Fe(0.1%)/Co(0.4%)-TiO_2 exhibited the highest photoactivity under visible light among all Fe/Co doped samples, about 65% RB was photodegraded in the solution within 4 h.

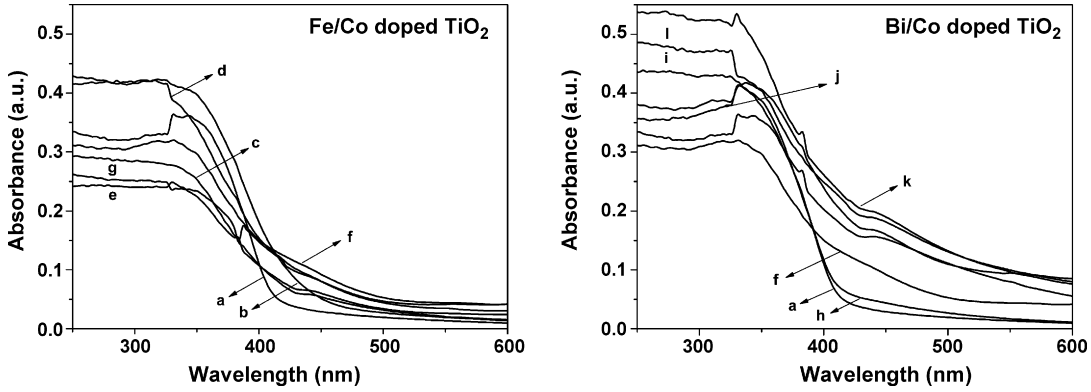

Fig. 4. UV–vis absorption spectra of as-prepared samples ((a) undoped TiO_2, (b) Fe(0.5%)-TiO_2, (c) Fe(0.4%)/Co(0.1%)-TiO_2, (d) Fe(0.25%)/Co(0.25%)-TiO_2, (e) Fe(0.1%)/Co(0.4%)-TiO_2, (f) Co(0.5%)-TiO_2, (g) Fe(0.5%)/Co(0.5%)-TiO_2, (h) Bi(0.5%)-TiO_2, (i) Bi(0.4%)/Co(0.1%)-TiO_2, (j) Bi(0.25%)/Co(0.25%)-TiO_2, (k) Bi(0.1%)/Co(0.4%)-TiO_2, (l) Bi(0.5%)/Co(0.5%)-TiO_2).

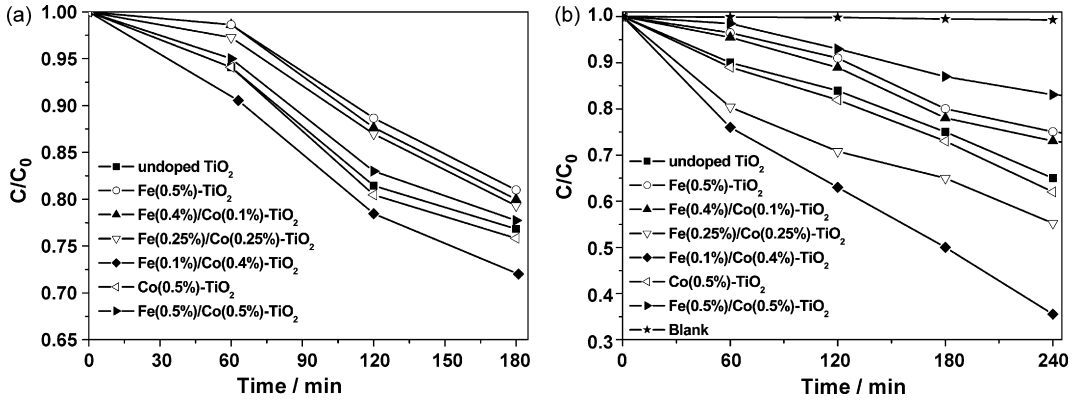

Fig. 5. Degradation profiles for Fe/Co doped TiO_2 under UV and visible light ((a) UV and (b) visible light).

The results may be explained by the cooperative effect of the two dopants on photoactivity. Such a cooperative effect can promote the charge carriers separation and interfacial charge transfer, thus improve the photoactivity of TiO_2 under visible light [22].

For Fe(III) monodoped TiO_2, Fe(III) ion can act as an electron trap as well as a hole trap, the recombination of the photoexcited charge carriers in the nanostructure can be restrained by Fe(III), so the charge carriers will have a long lifetime. In general, a relative increase in the concentration of the long-lived charge carriers results in a corresponding increase in photoactivity. But at the same time, the excess concentration of Fe would also trap too many charge carriers, the concentration of the available long-lived charge carriers decreased that could result in a decrease in photoactivity [5,22].

For Co(II) monodoped TiO_2, Co(II) mainly served as an electron trap [25]. The electrons, which were trapped on Co(II) sites, were subsequently transferred to the adsorbed oxygen to form superoxide radical ion O_2^- ($Co^{2+} + O_2 \rightarrow Co^{3+} + O_2^-$) [26]. Generally speaking, the faster transfer of electrons would speed up the process of photocatalytic reaction. But the results do not show obvious improvement in the photoactivity of Co(II) monodoped TiO_2 compared to undoped TiO_2. It may be due to the increased recombination of electrons with their mobile counterparts.

Thus, the monodoping with Fe(III) mainly improved charge carriers separation and Co(II) promoted interfacial charge transfer. But the codoping can improve these two processes simultaneously. In Fe/Co codoped TiO_2 system, Fe(III) may mainly serve as a hole trap and Co(II) as an electron trap. Such trappings restrained the recombination of charge carriers, and sped up interfacial charge transfer, which promoted the photoreaction. As a result, there was an optimal codoping concentration ratio (0.1%:0.4%) based on which the photoactivity of sample under visible light was the highest, and higher than that of Fe(III) or Co(II) monodoped TiO_2.

The degradation profiles for Bi/Co doped TiO_2 under UV and visible light are shown in Fig. 6. The photoactivity of Bi/Co doped TiO_2 under UV was slightly higher than that of Fe/Co doped TiO_2, but the results were still not satisfying. When the experiments were performed under visible light, Bi(0.25%)/Co(0.25%)-TiO_2 exhibited the best performance on the photodegradation of RB among all Bi/Co doped samples, but its photoactivity was lower than that of Fe(0.1%)/Co(0.4%)-TiO_2, though higher absorbency in the visible light region (Fig. 4).

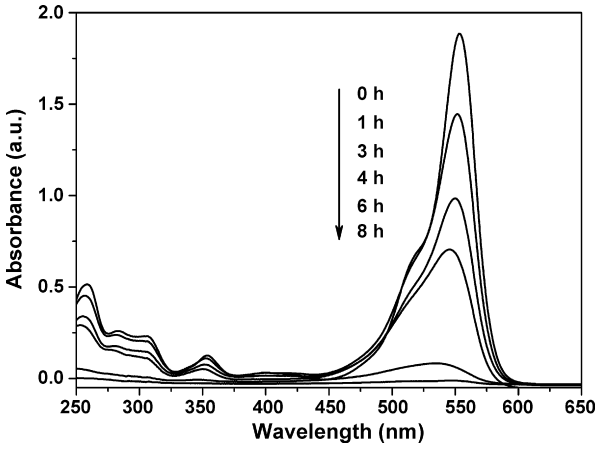

Fig. 7. UV–vis spectra of RB solutions collected at different intervals during the photodegradation in the presence of Fe(0.1%)/Co(0.4%)-TiO_2.

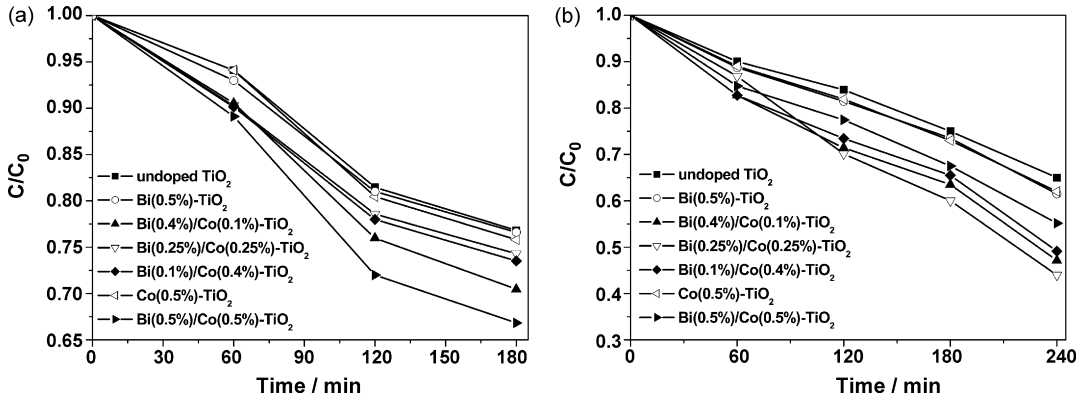

Fig. 6. Degradation profiles for Bi/Co doped TiO_2 under UV and visible light ((a) UV and (b) visible light).

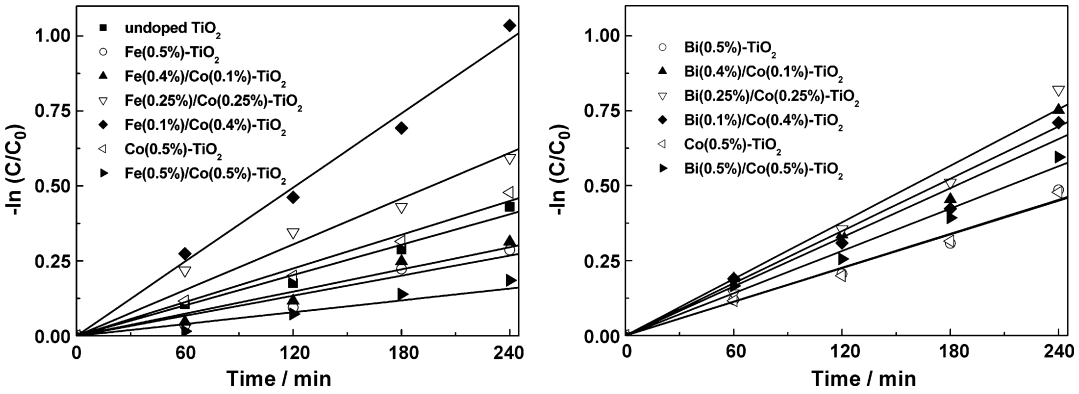

Fig. 8. Relationship between $-\mathrm{Ln}\,C/C_0$ and irradiation time.

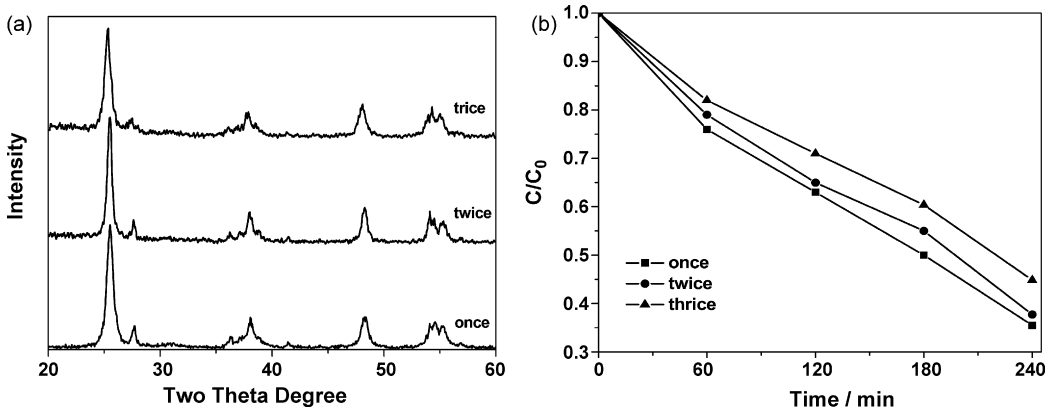

Fig. 9. The XRD patterns (a) and degradation profiles (b) under visible light for the reused Fe(0.1%)/Co(0.4%)-TiO_2.

For Bi(III) doped TiO_2, Bi(III) behaved as sites where electrons accumulated [27]. Better separation of electrons and holes on the modified TiO_2 surface allowed more efficient channeling of the charge carriers into useful reduction and oxidation reaction rather than recombination reaction.

In Bi/Co codoped TiO_2 system, both Bi(III) and Co(II) only improved interfacial charge transfer. So Bi/Co codoping cannot enhance the photoactivity of sample under visible light as much as Fe/Co codoping.

The UV–vis spectra recorded during the photodegradation of RB in the presence of Fe(0.1%)/Co(0.4%)-TiO_2 are shown in Fig. 7. In the process of photodegradation, we observed that the colour of solution weakened gradually. Moreover, the intensity of absorption spectra shown in Fig. 7 decreases with the increase in irradiation time, and all the absorption peaks disappear after 8 h. This implies that RB not only decolorized but also mineralized under visible light irradiation.

Fig. 8 shows the $-\mathrm{Ln}\,C/C_0$ of RB versus irradiation time t for the different catalysts. A approximate linear relationship of $-\mathrm{Ln}\,C/C_0$ versus t indicates that the photodegradation processes of RB tended to follow pseudo-first-order kinetic model in the presence of the catalysts studied in this paper. The apparent rate constants for Fe(0.1%)/Co(0.4%)-TiO_2 and Bi(0.25%)/Co(0.25%)-TiO_2 were estimated from the slope of $-\mathrm{Ln}\,C/C_0$ versus t to be 4.12×10^{-3} min^{-1} and 3.15×10^{-3} min^{-1}, respectively.

The best performing photocatalyst Fe(0.1%)/Co(0.4%)-TiO_2 was subjected to reuse in the presence of visible light irradiation. Fig. 9 shows that the phase structure of photocatalyst remained consistent, but the efficiency decreased about 5% after each reuse. The drop in the photoactivity of reused photocatalyst may be due to the adsorption of the original compound and/or by-products (adsorbed species) on the active sites of the catalyst surface, the reduction of the number of available photoactive sites resulted in the drop in the photoactivity [28]. Further use of the catalyst is also possible with lesser efficiency after the catalyst is filtered, washed and dried in sequence. However, we still continue to do further work to improve its recyclability from the viewpoint of application in practice.

4. Conclusions

In summary, Bi/Co and Fe/Co codoped TiO_2 were prepared by stearic acid gel method. XRD patterns showed that nanocrystals formed, and SEM micrographs showed that the samples consist of agglomerated particles. UV–vis spectra revealed that doped Co induced intense absorption of visible light, and the absorbency of as-prepared samples in the visible light region followed the order: Bi/Co codoped TiO_2 > Co monodoped TiO_2 > Fe/Co codoped TiO_2. The photoactivity of as-prepared samples was evaluated by the photodegradation of 20 mg/l RB solution under visible light. The results showed that monodoping Co or Bi was less effective for photoreaction, and monodoping Fe had a negative effect on the photoactivity of sample. But codoping Bi/Co or Fe/Co improved the photoactivity of as-prepared samples, and Fe(0.1%)/Co(0.4%)-TiO_2 showed the highest photoactivity under visible light among all as-prepared samples, though less absorbency of visible light. It can be explained by the reason that the Fe/Co codoping improved the charge carriers separation and interfacial charge transfer to achieve a higher utilization rate of visible light.

Acknowledgements

This work was financially supported by the National Natural Science Foundation of China (60374048) and Jilin Provincial Science and Technology Department (20060928). The authors are grateful to Lehui Zou and Lianxiang Yu for help.

References

[1] W. Zhao, C.C. Chen, X.Z. Li, J.C. Zhao, Photodegradation of sulforhodamine-B dye in platinized titania dispersions under visible light irradiation: Influence of platinum as a functional Co-catalyst, J. Phys. Chem. B 106 (2002) 5022–5028.
[2] A. Koca, M. Sahin, Photocatalytic hydrogen production by direct sun light from sulfide/sulfite solution, Int. J. Hydrogen Energy 27 (2002) 363–367.
[3] J. Wu, J.M. Lin, Y.B. Shu, T. Sato, Synthesis and photocatalytic properties of layered $HNbWO_6$/(Pt, $Cd_{0.8}Zn_{0.2}S$) nanocomposites, J. Mater. Chem. 11 (2001) 3343–3347.
[4] K. Domen, M. Hara, J.N. Kondo, T. Takata, A. Kudo, H. Kobayashi, Y. Inoue, New aspects of heterogeneous photocatalysts for water decomposition, Korean J. Chem. Eng. 18 (2001) 862–866.
[5] M.R. Hoffmann, S.T. Martin, W.Y. Choi, D.W. Bahnemann, Environmental applications of semiconductor photocatalysis, Chem. Rev. 95 (1995) 69–96.
[6] L. Zang, C. Lange, I. Abraham, S. Storck, W.F. Maier, H. Kisch, Amorphous microporous titania modified with platinum(IV) chlorides—a new type of hybrid photocatalyst for visible light detoxification, J. Phys. Chem. B 102 (1998) 10765–10771.
[7] H. Kisch, L. Zang, C. Lange, W.F. Maier, C. Antonius, D. Meissner, Modified, amorphous titania—a hybrid semiconductor for detoxification and current generation by visible light, Angew. Chem. Int. Ed. 37 (1998) 3034–3036.
[8] X.Z. Li, F.B. Li, Study of Au/Au^{3+}-TiO_2 photocatalysts toward visible photooxidation for water and wastewater treatment, Environ. Sci. Technol. 35 (2001) 2381–2387.
[9] A.V. Emeline, G.V. Kataeva, V.K. Ryabchuk, N. Serpone, Photostimulated generation of defects and surface reactions on a series of wide band gap metal-oxide solids, J. Phys. Chem. B 103 (1999) 9190–9199.
[10] D. Li, H. Haneda, S. Hishita, N. Ohashi, Visible-light-driven N–F-codoped TiO_2 photocatalysts. 1. Synthesis by spray pyrolysis and surface characterization, Chem. Mater. 17 (2005) 2588–2595.
[11] D. Li, H. Haneda, S. Hishita, N. Ohashi, Visible-light-driven N–F-codoped TiO_2 photocatalysts. 2. Optical characterization, photocatalysis, and potential application to air purification, Chem. Mater. 17 (2005) 2596–2602.
[12] D. Li, N. Ohashi, S. Hishita, T. Kolodiazhnyi, H. Haneda, Origin of visible-light-driven photocatalysis: a comparative study on N/F-doped and N–F-codoped TiO_2 powders by means of experimental characterizations and theoretical calculations, J. Solid State Chem. 178 (2005) 3293–3302.
[13] T. Ohno, T. Tsubota, M. Toyofuku, R. Inaba, Photocatalytic activity of a TiO_2 photocatalyst doped with C^{4+} and S^{4+} ions having a rutile phase under visible light, Catal. Lett. 98 (2004) 255–258.
[14] H.Q. Sun, Y. Bai, Y.P. Cheng, W.Q. Jin, N.P. Xu, Preparation and characterization of visible-light-driven carbon–sulfur-codoped TiO_2 photocatalysts, Ind. Eng. Chem. Res. 45 (2006) 4971–4976.
[15] D.G. Huang, S.J. Liao, J.M. Liu, Z. Dang, L. Petrik, Preparation of visible-light responsive N–F-codoped TiO_2 photocatalyst by a sol–gel-solvothermal method, J. Photochem. Photobiol. A 184 (2006) 282–288.
[16] C.C. Pan, J.C.S. Wu, Visible-light response Cr-doped $TiO_{2-X}N_X$ photocatalysts, Mater. Chem. Phys. 100 (2006) 102–107.
[17] P. Yang, C. Lu, N.P. Hua, Y.K. Du, Titanium dioxide nanoparticles co-doped with Fe^{3+} and Eu^{3+} ions for photocatalysis, Mater. Lett. 57 (2002) 794–801.
[18] Z.H. Yuan, J.H. Jia, L.D. Zhang, Influence of co-doping of Zn(II) + Fe(III) on the photocatalytic activity of TiO_2 for phenol degradation, Mater. Chem. Phys. 73 (2002) 323–326.
[19] W. Kallel, S. Bouattour, A.W. Kolsi, Structural and conductivity study of Y and Rb co-doped TiO_2 synthesized by the sol–gel method, J. Non Cryst. Solids 352 (2006) 3970–3978.
[20] H. Park, B. Neppolian, H.S. Jie, J.P. Ahn, J.K. Park, M. Anpo, D.Y. Lee, Preparation of bimetal incorporated TiO_2 photocatalytic nano-powders by flame method and their photocatalytic reactivity for the degradation of diluted 2-propanol, Curr. Appl. Phys. 7 (2007) 118–123.
[21] W.F. Yao, H. Wang, X.H. Xu, X.N. Yang, Y. Zhang, S.X. Shang, M. Wang, Preparation and photocatalytic property of La (Fe)-doped bismuth titanate, Appl. Catal. A 251 (2003) 235–239.
[22] D.W. Hwang, H.G. Kim, J.S. Lee, J. Kim, W. Li, S.H. Oh, Photocatalytic hydrogen production from water over M-doped $La_2Ti_2O_7$ (M = Cr, Fe) under visible light irradiation ($\lambda > 420$ nm), J. Phys. Chem. B 109 (2005) 2093–2102.
[23] S.S. Srinivasan, J. Wade, E.K. Stefanakos, Y. Goswami, Synergistic effects of sulfation and co-doping on the visible light photocatalysis of TiO_2, J. Alloy. Compd. 424 (2006) 322–326.
[24] C. Kormann, D.W. Bahnemann, M.R. Hoffmann, Environmental photochemistry: is iron oxide (hematite) an active photocatalyst? A comparative study: α-Fe_2O_3, ZnO, TiO_2, J. Photochem. Photobiol. A 48 (1989) 161–169.
[25] W.Y. Choi, A. Termin, M.R. Hoffmann, The role of metal ion dopants in quantum-sized TiO_2: correlation between photoreactivity and charge carrier recombination dynamics, J. Phys. Chem. 98 (1994) 13669–13679.
[26] M.A. Barakat, H. Schaeffer, G. Hayes, S. Ismat-Shah, Photocatalytic degradation of 2-chlorophenol by Co-doped TiO_2 nanoparticles, Appl. Catal. B 57 (2005) 23–30.
[27] S. Rengaraj, X.Z. Li, Enhanced photocatalytic reduction reaction over Bi^{3+}-TiO_2 nanoparticles in presence of formic acid as a hole scavenger, Chemosphere 66 (2007) 930–938.
[28] C.G. Silva, W.D. Wang, J.L. Faria, Photocatalytic and photochemical degradation of mono-, di- and tri-azo dyes in aqueous solution under UV irradiation, J. Photochem. Photobiol. A 181 (2006) 314–324.